

JLab C100 Cryomodule Cavity Characterization

Qiang Du, Larry Doolittle, Gang Huang, Carlos Serrano Pareja, and Alessandro Ratti

Lawrence Berkeley National Lab

Trent Allison and Ramakrishna Bachimanchi

Thomas Jefferson National Lab

August 12, 2013

1 Introduction

This document describes the algorithm and implementation of automatic cavity characterization using I & Q waveforms from LLRF controllers in JLab 12GeV cryomodule commissioning, including:

Pulse Mode falling edge cavity analysis This method uses falling edge analysis in pulse mode to determine Q_L and Q_{FP} so that cavity gradient could be calculated by probe signal power in CW mode.

Burst mode chirp response cavity analysis This method uses chirp signal generated by LLRF to drive the cavity ¹ and analysis the transmitted signal waveforms to determine the cavity bandwidth, cavity detune, external gain and phase offset.

2 Cavity model

The following math is to derive a general equation for both fitting methods.

The high Q cavity could be modeled as a general second order dynamic system, or a band pass filter, with possible non-zero initial state. ²

The transfer function of the cavity in Laplace domain is:

$$H(s) = \frac{2\alpha s}{s^2 + 2\alpha s + \omega_0^2}$$

where α is the attenuation factor, ω_0 is the central resonance frequency at $2\pi \cdot 1497$ MHz.

In this case the system is under damped since the damping ratio $\zeta = \frac{\alpha}{\omega_0} \ll 1$, so $H(s)$ has two conjugate poles at the left half of s -plane, located at $\lambda_{1,2}$, very close to imaginary axis. $\lambda_{1,2}$ are the two roots of the characteristic equation:

$$\lambda_{1,2} = -\alpha \pm j\omega_d, \quad \omega_d = \sqrt{\omega_0^2 - \alpha^2}, \quad \zeta = \frac{1}{\omega_0\tau} = \frac{1}{2Q}$$

¹Supported by Firmware version 43 or later

² Due to Lorentz force detuning effect, ω_0 will change due to the energy stored in the cavity (experiment shows ~ 300 Hz in normal condition), and the classic second order dynamic system response does not exactly apply any more. But the relations of coefficients still apply.

where ω_d is defined to be the *damped natural frequency*,

The full bandwidth of the cavity is measured between the 3dB points, which could be calculated as

$$\Delta\omega = 2\alpha = \frac{2}{\tau} = \frac{\omega_0}{Q}$$

Note that the time constant calculated by the decay of $P(t)$ is $\tau_p = \frac{1}{2}\tau$ since $P(t) \propto V^2(t)$.

The FCC LLRF controller mixes the cavity response signal with the local oscillator frequency $\omega_{LO} = 2\pi \cdot 1427$ MHz, so the original two conjugate poles $\lambda_{1,2}$ become four poles:

$$\begin{cases} \lambda_{11,12} &= -\alpha + j(\omega_{LO} \pm \omega_d) \\ \lambda_{21,22} &= -\alpha - j(\omega_{LO} \mp \omega_d) \end{cases}$$

When studying the IF signal, the high frequency components are filtered out, so we have only two conjugate poles at $\lambda_{12,21} = -\alpha \pm j(\omega_{LO} - \omega_d)$ instead. And the zero of $H(s)$ also moved to position at $\pm j\omega_{LO}$ which are also filtered out. Meanwhile, the amplitude of response will also be split to half by the filter to get a system gain of α .

The FPGA then converts the I&Q sampled IF signal to base band in digital region. By adding the quadrature part, the process is equivalent to a mixing with a complex signal $e^{j(\omega_0 - \omega_{LO})t}$, which would move the poles to base band and cancel out a conjugate pole to get a single complex pole base band system function $H_2(s)$. Note the gain would be back to 2α again.

$$H_2(s) = \frac{2\alpha}{s - (-\alpha + j\omega_{cd})}, \quad \omega_{cd} = \omega_0 - \omega_d$$

Here $\frac{1}{2\pi}\omega_{cd}$ is defined as the cavity detune frequency. In order to study non-zero state system response, we can re-write this to a first order differential equation in general case:

$$\frac{dy(t)}{dt} - (-\alpha + j\omega_{cd})y(t) = 2\alpha \cdot x(t) \quad (1)$$

Where $x(t)$ is the driver signal to the cavity which includes the external gain and phase delay relative to LLRF output. This equation is identical to the basic cavity field equation described in reference [2].

3 Pulsed mode falling edge cavity analysis

This analysis studies the zero input response of cavity after falling edge of drive signal, as $x(t) = 0$ in equation 1.

It is capable of determining the cavity bandwidth, loaded Q , cavity stored energy before falling edge U , field probe quality factor Q_{FP} , and cavity gradient E by the waveforms of reflected power P_r , the power of transmitted signal P_t , forward power signal P_f from JLab Field Control Chassis LLRF controllers, and known cavity characteristic constants & attenuation calibration factors.

3.1 Signal definitions

Summary of interested signals are listed in table 1. Typical values are collected at 1L23-1 when gradient is ~ 10 MV/m.

Symbol	Typical Value	Unit	Description	Comment
P_f	~ 500	Watt	Forward power	WF08
P_r	$< P_f$	Watt	Reflected power	WF14/15
P_t	~ 0.05	Watt	Transmit power	WF00/01
C_f	~ 54	dB	Attenuation of forward power	
C_r	~ 54	dB	Attenuation of reflected power	
r/Q	868	Ω/m	Shunt impedance	cavity constant
L	0.7	m	Electrical length	cavity constant
f_0	1497	MHz	Cavity tuned frequency	cavity constant
τ	3.5	ms	Cavity decay time constant	
U	~ 5.0	J	Stored energy	Output
E	10	MV/m	Cavity gradient	Output
Q_L	$\sim 3.0 \times 10^7$		Loaded Q	Output
Q_{FP}	$\sim 1.0 \times 10^{12}$		Field Probe coupler Q	Output
Q_{FPC}	$\sim Q_L$		Fundamental Power Coupler Q	Output
Q_0	$> 2.5 \times 10^{11}$		Intrinsic Q	measured separately
GGPRB	5×10^7		Ratio between LabVIEW E to GMES	initial 1

Table 1: JLab C100 Cavity analysis signal list

3.2 Theory

The general definition of quality factor applies to this study:

$$Q = \frac{\omega U}{P}$$

where $2\pi \cdot \omega$ is the resonant frequency, U is stored energy, and P is energy dissipated per cycle. Q can be defined at different view of points according to different power dissipation definition.

According to [1], the extended equations for cavity analysis are summarized as below:

$$\begin{aligned}
Q_L &= \frac{\omega_0}{\Delta\omega} = 4\pi f_0 \tau = 2\pi f_0 \tau_p \\
\tau &= \frac{2}{\Delta\omega} = \frac{1}{2\pi f_{1/2}} \\
U &= \int_0^\infty P_r(t) dt = \int_0^\infty P_r(t_0) e^{-\frac{t}{\tau_p}} dt = P_{RFL}(t_0) \cdot \tau_p \\
E &= \sqrt{2\pi f_0 U \cdot \frac{r/Q}{L}} \\
Q_{FP} &= \frac{E^2}{P_{TRAN}} \cdot \frac{L}{r/Q} \\
\frac{1}{Q_L} &= \frac{1}{Q_0} + \frac{1}{Q_{FP}} + \frac{1}{Q_{FPC}}, \quad Q_L \simeq Q_{FPC} \\
GGPRB &= \sqrt{\frac{r/Q}{L}} \cdot Q_{FP}
\end{aligned}$$

3.3 Waveform acquisition and calibration

All input waveforms are sampled by LLRF controller and are available by EPICS CA records. Sampling period is $R101TRGS1r/R101TRGS1.ASLO/4$ clock cycles, where $TRGS1.ASLO = 1000/f_{clk}$,

and $f_{\text{clk}} = 56\text{MHz}$.

FPGA circular buffer has 8192 samples while IOC reads every 4 samples to get 2048 points. `caget` gets the leading 2000 points. Waveform acquisition is triggered (mode TRGD2=2) to include $4 \times \text{TRGD1}$ points after falling edge. So we know the falling edge at $2048 - \text{TRGD1}$ point. Another way is to search the negative peak of differential GASK signal and match the peak location to reflected power waveform. Real data shows equivalent results using both methods by starting analysis from 0.1ms after the falling edge.

A `bash` script `savewf.sh` is written to grab all 16 waveforms and assemble it into a single datafile for online and off line analysis.

Waveforms from LLRF chassis are calibrated by a testing stand with power meters to match CORDIC output counts to real watts by interpolation of a 256 points calibration table. Note that there is also a CORDIC gain of 1.647 to convert from $\sqrt{I^2 + Q^2}$ to the count for interpolation.

3.4 Attenuation calibrations

From cavity front end coupler to FCC LLRF chassis, there are waveguide coupler, cables, jumpers and external attenuations that should be calibrated for calculation.

The calibration factors at 1L23 cavity 1 for both LabVIEW test stand and EPICS PVs are compared in table 2. A mismatch of about 1.8dB is found between them, which may be a main factor of the measurement difference.

Attenuation Factors	LabVIEW test stand (dB)	EPICS PV (dB)	Error(dB)
Waveguide coupler	50.15	~ 50	
Cable	6.12	1.37	
Jumper	0	0.2	
Extra	0	3.02	
Total	56.37	54.59	1.78

Table 2: 1L24-1 reflected signal calibration factor mismatch

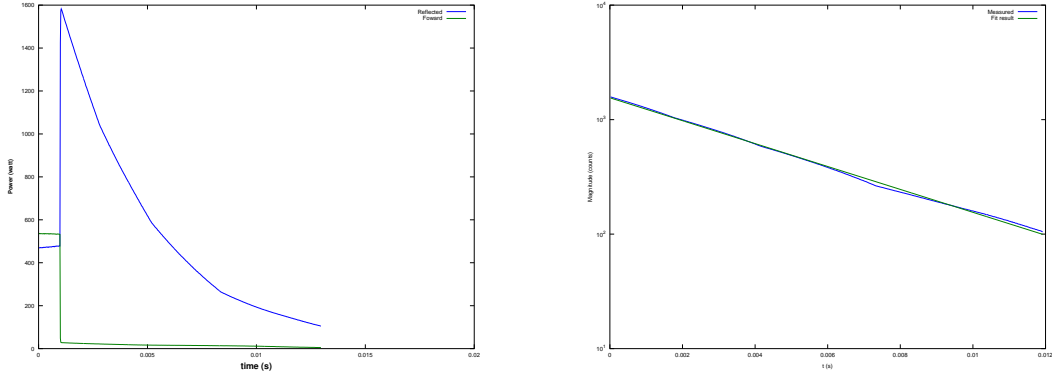
3.5 Offline analysis by OCTAVE/Matlab

Refer to `freq2.m`. Figure 1 shows waveform from LLRF through EPICS PV for cavity 1L24 and the fitting result.

The measured results are shown in table 3 in compare with ELOG Q_L or EPICS GMES reading in SEL mode.

Value	Measured	Actual/ELOG	Error
$\Delta\omega$	36.66 Hz		
Q_L	4.08×10^7	4.53×10^7	-9.9%
U	6.33 J		
Q_{FP}	1.80×10^{12}		
E	8.59 MV/m	12.59 MV/m	-31.8% or -1.66 dB

Table 3: Offline Decay waveform analysis results for 1L24-1



(a) forward and reflected power waveform (b) reflected power decay waveform fitting

Figure 1: Falling edge cavity analysis on 1L24-1

3.6 On line analysis by Python

The OCTAVE code was re-written into Python script `cavity_ana_epics.py` so that we can work with python module `pyepics` with `caget` to do on line analysis. The algorithm and results are verified identical for both methods. On line measurements was done on Aug 01 2013 with the results in table 4 on 1L23-1, and table 5 on 1L23-2.

Value	Measure 1	Measure 2	Measure 3	reading in SEL	Error
$\frac{1}{2\pi}\Delta\omega$ (Hz)	45.89	47.73	46.78	2.95	8.5%
$Q_L (\times 10^7)$	3.26	3.14	3.20		
U (J)	5.27	5.18	5.21		
$Q_{FP} (\times 10^{12})$	1.51	1.49	1.49		
P_f (Watt)	436.8	435.4	435.4	9.56	-18.4%
P_t (Watt)	0.033	0.033	0.033		
E (MV/m)	7.84	7.78	7.79		
GGPRB ($\times 10^7$)	4.33	4.30	4.31	5.26	-17.8%

Table 4: Decay waveform analysis results for 1L23-1 at 2013-08-01 22:18

Value	Measure 1	Measure 2	Measure 3	reading in SEL	Error
$\frac{1}{2\pi}\Delta\omega$ (Hz)	48.08	48.38	48.34	2.99	3.6%
$Q_L (\times 10^7)$	3.11	3.09	3.10		
U (J)	4.43	4.45	4.44		
$Q_{FP} (\times 10^{12})$	0.86	0.86	0.87		
P_f (Watt)	423.9	420.9	424.5	9.52	-24.3%
P_t (Watt)	0.048	0.048	0.048		
E (MV/m)	7.19	7.19	7.20		
GGPRB ($\times 10^7$)	3.27	3.27	3.28	4.34	-24.4%

Table 5: Decay waveform analysis results for 1L23-2 at 2013-08-01 22:09

The 18% error between measured gradient and EPICS reading may be caused by calibration

factor ~ 2 dB mismatch described at table 2.

4 Burst mode chirp response cavity analysis

We can derive the time difference equation from 1:

$$\frac{2}{T} (\mathbf{y}(n) - \mathbf{y}(n-1)) - \lambda (\mathbf{y}(n) + \mathbf{y}(n+1)) = \mathbf{g} (\mathbf{u}(n) + \mathbf{u}(n+1)), \quad \lambda = -\alpha + j\omega_{cd}, \mathbf{g} = |g|e^{j\phi_g}$$

where $\mathbf{y}(n), \mathbf{u}(n)$ is the sampled vector signal of $y(t), u(t)$ with sampling rate $\frac{1}{T}$, $\mathbf{u}(t)$ is the output DAC vector signal from LLRF, and \mathbf{g} is the external gain and phase delay introduced by cable, klystron, cavity, etc., all in complex form.

The goal of this analysis is to fit the unknown λ and \mathbf{g} using linear least square method.

For this overdetermined system $\mathbf{X}\beta = \mathbf{y}$, one should provide the matrix \mathbf{X} with each column linearly independent in the sense of solving the quadratic minimization. So we can re-write the above difference equation in the form of matrix:

$$\begin{bmatrix} \mathbf{X}(1+z^{-1}) & \mathbf{U}(1+z^{-1}) \end{bmatrix} \begin{bmatrix} \lambda & \mathbf{g} \end{bmatrix} = \begin{bmatrix} \mathbf{X}(1-z^{-1}) \cdot \frac{2}{T} \end{bmatrix} \quad \mathbf{X}, \mathbf{U} \in \mathbb{C}^{2000 \times 1}, \quad \lambda, \mathbf{g} \in \mathbb{C}^{1 \times 1}$$

λ, \mathbf{g} could then be solved by pseudo inverse of the left matrix:

$$\begin{bmatrix} \lambda & \mathbf{g} \end{bmatrix} = \begin{bmatrix} \mathbf{X}(1+z^{-1}) & \mathbf{U}(1+z^{-1}) \end{bmatrix}^+ \begin{bmatrix} \mathbf{X}(1-z^{-1}) \end{bmatrix} \cdot \frac{2}{T}$$

4.1 Off line analysis by OCTAVE/Matlab

Refer to `chirp_test.m` and `freq2.m`. Off line analysis shows cavity 1L23-1 has bandwidth of 40.55 Hz, cavity detune -260.6 Hz, external gain 18.23, and phase offset -171.4° based on data took at 2013-08-01 22:32.

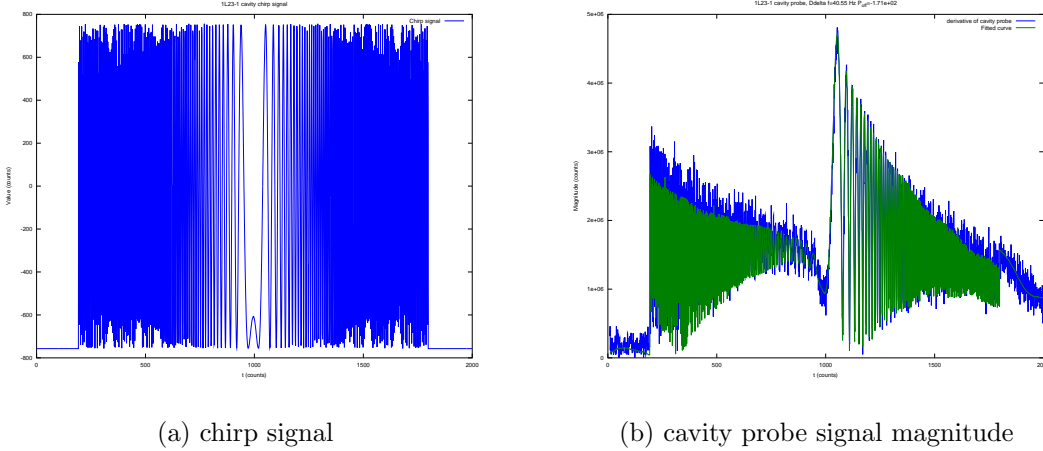


Figure 2: derivative of cavity probe and fitted curve

4.2 On line analysis by Python

Refer to `cavity_ana_epics.py` in function `chirp_ana_ld`. Table 6 and 7 summarize the chirp signal cavity analysis on line test results. The fitting shows that $\Delta\omega$ is smaller than known value but phase offset and frequency offset values are quite accurate. Further study is needed to improve the fitting.

Value	Measure 1	Measure 2	Measure 3	Known value	Error
$\frac{1}{2\pi}\Delta\omega$ (Hz)	39.52	41.26	40.60	46.78	-13.5%
$\frac{1}{2\pi}\omega_{cd}$ (Hz)	267.6	293.4	343.0	284	6.1%
Gain	19.36	18.53	18.88		
Phase offset ($^{\circ}$)	169.4	169.4	169.6	169 ± 11	0.3%

Table 6: Burst mode waveform analysis results for 1L23-1 at 2013-08-01 18:19

Value	Measure 1	Measure 2	Measure 3	Known value	Error
$\frac{1}{2\pi}\Delta\omega$ (Hz)	39.65	39.44	39.36	48.26	-18.2%
$\frac{1}{2\pi}\omega_{cd}$ (Hz)	-1397.3	-1404.6	-1400.8	-1311	6.8%
Gain	27.11	27.13	27.16		
Phase offset ($^{\circ}$)	-6.9	-6.9	-6.2	-6.6 ± 9	0.1%

Table 7: Burst mode waveform analysis results for 1L23-2 at 2013-08-01 22:25

4.3 Data fitting by C/C++

Refer to `cavity_fit.cc` using `newmat` library, `cavity_fit2.cpp` using library `armadillo` for matrix manipulations, or `cavity_fit_r.c` without external math libs. Those files are not complete for real data analysis yet. They should be able to run on either IOC or EPICS server.

5 Conclusion

We have implemented two methods for automatic cavity characterization using JLab LLRF controller waveform samples and known calibration factors. The cavity gradient, Q_L and Q_{FP} are measured by a falling edge decay method, and the cavity bandwidth and detune, phase offset are fitted using a chirp stimulation signal analysis.

Results show that a mismatch of ~ -2 dB is founded between the measurement gradient and EPICS PV `GMES` reading, which may possibly be caused by a calibration factor difference used by LabVIEW test stand and EPICS IOC. Chirp signal analysis shows good accuracy on cavity detune and phase offset measurement. Both analysis results are stable, and are implemented in a Python script that can be run lively on any EPICS operation servers at JLab.

6 Acknowledgments

The authors would like to thank Michael Drury, Larry King, George Lahti, Tom Powers and all other colleagues at Jefferson Lab for their kindly help and great support to this work.

References

- [1] Tom Powers, *Theory and Practice of Cavity RF Test Systems*, Proceedings of the 12th International Workshop on RF Superconductivity, Cornell University, Ithaca, New York, USA, 2005
- [2] Larry Doolittle, *Analysis of Burst Mode Cavity Tuning Data*, JLab Tech note 99-011, April 23, 1999